Structures of the intermediates in the catalytic cycle of mitochondrial cytochrome c oxidase

Wikström, Mårten

2023-04-01

Wikström , M , Gennis , R B & Rich , P R 2023 , ' Structures of the intermediates in the catalytic cycle of mitochondrial cytochrome c oxidase ' , Biochimica et Biophysica Acta. Bioenergetics , vol. 1864 , no. 2 , 148933 . https://doi.org/10.1016/j.bbabio.2022.148933

http://hdl.handle.net/10138/352009
https://doi.org/10.1016/j.bbabio.2022.148933

BBA - Bioenergetics 1864 (2023) 148933

Contents lists available at ScienceDirect

BBA - Bioenergetics

journal homepage: www.elsevier.com/locate/bbabio

Structures of the intermediates in the catalytic cycle of mitochondrial cytochrome *c* oxidase

Mårten Wikström [a,*], Robert B. Gennis [b], Peter R. Rich [c]

[a] HiLIFE Institute of Biotechnology, University of Helsinki, Helsinki, Finland
[b] Department of Biochemistry, University of Illinois at Urbana-Champaign, Urbana, IL, USA
[c] Glynn Laboratory of Bioenergetics, Institute of Structural and Molecular Biology, University College London, London, UK

ARTICLE INFO

Keywords:
Cell respiration
Oxygen reduction
Heme-copper oxidases
Respiratory chain

ABSTRACT

Cytochrome *c* oxidase is the terminal complex of the respiratory chains in the mitochondria of nearly all eukaryotes. It catalyzes the reduction of molecular O_2 to water using electrons from the respiratory chain, delivered via cytochrome *c* on the external surface of the inner mitochondrial membrane. The protons required for water formation are taken from the matrix side of the membrane, making catalysis vectorial. This vectorial feature is further enhanced by the fact that the redox catalysis is coupled to the translocation of protons from the inside to the outside of the inner mitochondrial membrane. We are dealing with a molecular machine that converts redox free energy into a protonmotive force (pmf). Here, we review the current extensive knowledge of the structural changes in the active heme-copper site that accompany catalysis, based on a large variety of time-resolved spectroscopic experiments, X-ray and cryoEM structures, and advanced computational chemistry.

1. Cell respiration

In eukaryotes, cell respiration occurs exclusively in the mitochondria, more specifically in the inner mitochondrial membrane. With very few exceptions, the actual consumption of O_2 is catalyzed by the terminal enzyme complex of the respiratory chain, cytochrome oxidase or cytochrome *c* oxidase (C*c*O). C*c*O catalyzes the 4-electron reduction of O_2 to water, and the considerable free energy change of this reaction is used to drive charges (and protons specifically) across the membrane to generate a protonmotive force (pmf).

$$4\ \text{cyt}\ c_{red} + 8\ H^+_{in} + O_2 \rightarrow 4\ \text{cyt}\ c_{ox} + 4\ H^+_{out} + 2\ H_2O$$

How this enzyme converts chemical redox free energy into a transmembrane voltage and pH difference has motivated mechanistic studies since the 1970s.

C*c*O is for all practical purposes functionally identical in all eukaryotes. By contrast, in prokaryotes the variability in respiratory chains is considerable [1]; many prokaryotes can express different combinations of respiratory chain complexes depending on growth conditions, and this variability extends to the terminal oxidases, which can oxidize either cytochrome *c* (as in mitochondria) or a quinol. The bulk of the bacterial oxygen reductases are structurally and functionally related to the mitochondrial C*c*O. These enzymes belong to the large family of heme-copper oxygen reductases, which all contain a binuclear center (BNC) that consists of a heme group where the heme iron is usually within 5 Å of a copper ion (Fig. 1) [2–9] and which is the active site where O_2 binds and is reduced. A second heme, which is low spin with bis-histidine axial ligands, is adjacent to the heme of the BNC and is the immediate electron donor to the active site.

Whereas prokaryotic oxygen reductases utilize a variety of heme chemical variants (e.g. heme A, heme B, heme O) at these two sites [1,10], in eukaryotic C*c*Os both sites always contain heme A. These are referred to as heme *a* and heme a_3, the latter denoting the O_2-binding heme of the BNC, and mitochondrial C*c*O is often called cytochrome aa_3.

The copper of the BNC (called Cu_B) is bonded by three histidine ligands, one of which forms a unique covalent bond to a tyrosine residue [2]. This is a fully conserved special feature in all heme-copper oxygen reductases [11,12].

The superfamily of heme-copper oxygen reductases can be subdivided minimally into A-, B- and C-families [13–15]. The mitochondrial C*c*Os are all in the A-family and closely resemble the bacterial A-family oxygen reductases. In this paper we focus on the catalytic intermediates in the oxygen reduction cycle of the mitochondrial C*c*O. Many experiments have demonstrated the great similarities between the eukaryotic

* Corresponding author.
E-mail addresses: marten.wikstrom@helsinki.fi (M. Wikström), r-gennis@illinois.edu (R.B. Gennis), prr@ucl.ac.uk (P.R. Rich).

https://doi.org/10.1016/j.bbabio.2022.148933
Received 10 August 2022; Received in revised form 30 October 2022; Accepted 7 November 2022
Available online 17 November 2022

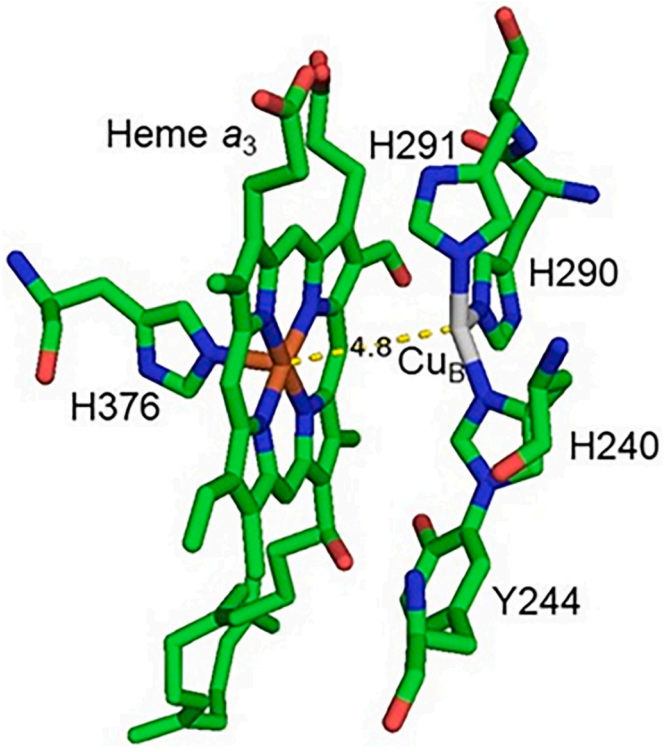

Fig. 1. The binuclear center of bovine CcO. The coordinates are taken from the published structure of fully oxidized bovine CcO at 1.5 Å resolution (PDB 5B1A; [91]). Heme a_3 is ligated by a single histidine; Cu_B is ligated by three histidines. One of the Cu_B histidines (H240) is covalently linked to the catalytically important Y244. The center-center Fe-Cu distance is 4.8 Å. See text for redox, ligand and protonation states of the intermediates formed during catalysis.

CcO and its prokaryotic A-family counterparts, and this review will draw from results obtained with these bacterial homologues when applicable. The bacterial enzymes offer experimental advantages due to greater structural simplicity (fewer subunits) and the availability of site-directed mutagenesis.

The bacterial A-family heme-copper oxygen reductases contain only four subunits compared to as many as 13 subunits for the mitochondrial enzyme. Three of the subunits of the bacterial enzymes are homologous with the three largest subunits of the mitochondrial CcOs (often called subunits I, II and III). In mitochondria, these subunits are encoded by mtDNA. The three-dimensional structure of mitochondrial CcO from bovine heart [2,16–18] has been solved, as have the homologous structures of the A-type CcOs from *Paracoccus denitrificans* [19], *Rhodobacter sphaeroides* [5,20], and the quinol oxidases from *Escherichia coli* and *Bacillus subtilis* [8,9,21]. More recently, eukaryotic CcO structures from other organisms have been solved by cryoEM, albeit at lower resolution, including human [22,23], ovine [24], yeast [25,26] and higher plant [27] CcOs.

The approach in this paper will be brief and focused on the current understanding of the catalytic intermediate structures. For more extensive historical reviews the reader is referred to [28–34].

Four electrons (and four protons) are required to reduce O_2 to 2 H_2O. Under physiological conditions in intact cells, the rate of reduction of CcO by cyt c_{red} is slow so that after each of the four one-electron reduction steps CcO has time to form a transient, metastable intermediate before the next electron is delivered. Each of the four one-electron transfers is further coupled to the translocation of one proton across the membrane, i.e., the proton pump activity. Fig. 2 summarizes the present view of the catalytic cycle of CcO from the point of view of the intermediate structures of the BNC, each of which will be discussed separately below.

2. The fully reduced and mixed valence states of CcO

The mitochondrial CcO and all bacterial A-family cytochrome *c* oxidases contain 4 redox-active metal centres. In addition to the already mentioned heme *a*, heme a_3, and Cu_B, they contain Cu_A which is the initial electron acceptor from reduced (ferrous) cytochrome *c*. Whilst Cu_A is a dinuclear copper centre, it is a one-electron donor/acceptor, shuttling between the forms Cu[*I*]Cu[II] (oxidized) and Cu[*I*]Cu[I] (reduced). Thus, the fully reduced (**FR**) state of CcO has 4 electrons

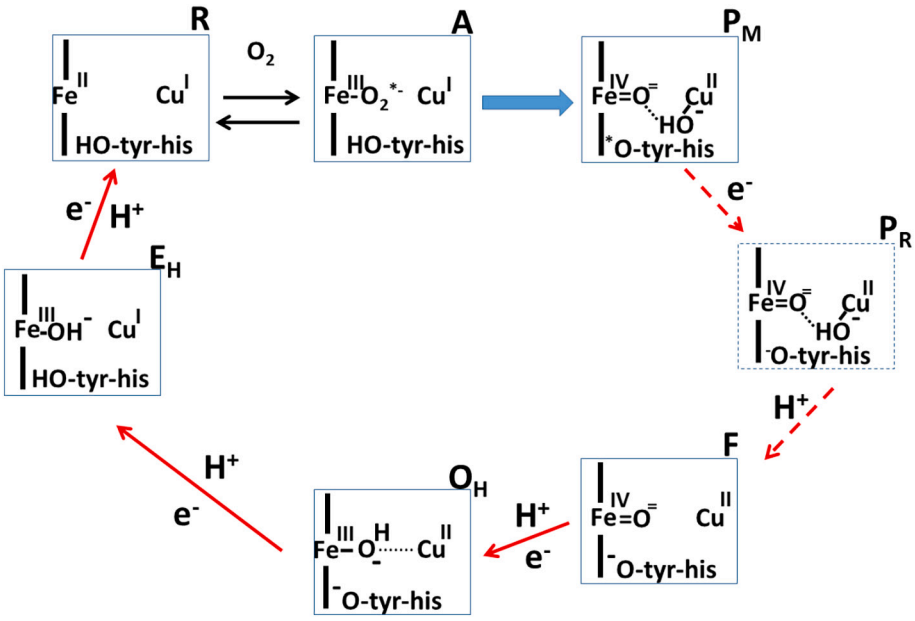

Fig. 2. Catalytic cycle. The rectangles describe the states of the binuclear centre. The name of each state is indicated near the upper right corner. The proximal histidine ligand of heme a_3 and the three histidine ligands of Cu_B are not shown for simplicity. HO-Tyr-His refers to the conserved tyrosine that is covalently bonded to one of the three histidine ligands of Cu_B. $^-$O-Tyr-His and *O-Tyr-his refer to the respective tyrosinate and neutral tyrosine radical forms. We have also denoted the free radical superoxide of state A with * for consistency. Note that the structures of the **F** and $\mathbf{O_H}$ states shown have alternatives where an electron from the tyrosinate is displaced to the copper (see text). Red arrows show the four partial reactions in which one electron and one proton is brought to the BNC, and where one additional proton is translocated from the matrix to the intermembrane space (not shown). Dashed red arrows show the formation and decay of the special intermediate $\mathbf{P_R}$ outlined by a dashed rectangle (see text). Formation of water is not shown for clarity, but is assumed to occur in the steps forming intermediates **F** and **R**, respectively. The blue arrow shows the essentially irreversible reaction step ($\Delta G \sim -5$ kcal/mol) in which bound O_2 is effectively fully reduced by four electrons (to an oxide bound to ferryl iron and a hydroxide bound to Cu_B). (For interpretation of the references to colour in this figure legend, the reader is referred to the web version of this article.)

readily available from the four redox-active metals, [Cu_A(I), Fe_a(II), Fe_{a3}(II), Cu_B(I)], sufficient to react with O_2 to form 2 H_2O in a single turnover without requiring the addition of cyt c_{red}. Studying the mechanism of this reaction is one important approach to unraveling the catalytic mechanism and the characteristics of the transient intermediate states. It should be noted that the **FR** state is an experimental convenience and that this state is not expected normally under physiological conditions.

An important variation to studying the reaction of O_2 with the **FR** state is to begin with a 2-electron reduced enzyme, called the mixed-valence (**MV**) enzyme: Cu_A(II), Fe_a(III), Fe_{a3}(II), Cu_B(I). The **MV** state also reacts with O_2, in this case forming an oxygen adduct called $\mathbf{P_M}$ (see below). Finally, note that we use the term **R** state for the fully reduced state of the BNC itself (Fe[*II*]Cu[I]; Fig. 2).

3. Compound A and the apparent K_M for oxygen

In the mid-1970s there were already kinetic/spectrophotometric indications of the presence of an 'oxygen adduct' as the primary enzyme-substrate complex in the reaction of reduced C*c*O with O_2. In 1975 Chance, Saronio and Leigh [35] demonstrated this intermediate at low temperatures by an ingenious triple-trapping technique, and called it Compound **A**. Compound **A**, the spectrum of which closely resembles that of the classical ferrous heme a_3-CO adduct with peaks at 590 and 430 nm in reduced-*minus*-oxidized difference spectra, was later found also in room temperature experiments. Both at low and room temperatures the binding of O_2 to the reduced active site was, perhaps surprisingly, found to be very weak, with a dissociation constant as high as ca. 0.25 mM [35–37]. This is in apparent contradiction to the observed steady-state kinetics oxygen affinity in cell respiration, the apparent K_M being well below 1 μM under most conditions [38]. However, as originally suggested by Chance et al. [35], this apparently high affinity is caused by very fast kinetic trapping of the bound O_2, relative to the overall turnover rate, a concept that was confirmed in room temperature experiments [36,37].

Although Compound **A** is formally a dioxygen adduct where O_2 is bound to the ferrous iron of heme a_3, quantum-chemical calculations and vibrational spectroscopy [39–42] have shown that the actual structure resembles those of oxyhemoglobin and oxymyoglobin [43,44] in which an electron is strongly displaced from the heme iron onto the O_2 ligand, to the extent that the actual structure is best described as a ferric-superoxide complex. In other words, what is formally

$$\mathrm{Fe(II) - O_2\ Cu(I)}$$

$$\mathrm{His - TyrOH}$$

is more accurately represented as (**1**), below,

1. Fe[III]-O_2^{*-} Cu[I]
   His-Tyr-OH

Please note that in this structure of the BNC, as in those to follow, the proximal ligand of heme iron and the porphyrin ring, as well as the three histidine ligands of Cu_B are not shown for simplicity. In (**1**), the Fe and Cu refer, respectively, to the iron in heme a_3 and to Cu_B, and the His-Tyr-OH refers to the unique crosslinked His-Tyr cofactor that is ligated to Cu_B in all heme-copper oxygen reductases.

4. The P intermediates: $\mathbf{P_M}$ and $\mathbf{P_R}$

It would be reasonable to assume that the next intermediate would result from the transfer of a second electron into the oxygen species, forming a peroxide (two-electron reduced O_2: O_2^{2-} or HOO^-) ligated to ferric heme a_3, with this second electron likely coming from Cu_B [45,46]. Alternatively, the second electron (and a proton) could be donated by the tyrosine in the active site [46] yielding a neutral tyrosyl radical. The expectation of a peroxy species as the intermediate following compound **A** (**1**) is reflected in the name of the intermediate observed, the **P** state. However, a true peroxide intermediate has never been detected. Thus, if a peroxide species is formed directly from compound **A**, it must be converted very rapidly to the observed intermediate, **P**.

The low temperature studies by Chance et al. [33] of the reaction of O_2 with the 2-electron reduced mixed valence state (**MV**) of C*c*O showed initially the formation of Compound **A** (**1**) which was subsequently converted to a species characterized optically by peaks at 607 nm and 430 nm in the difference spectrum versus the oxidized enzyme. This was called Compound **C**, and subsequently re-named as the $\mathbf{P_M}$ state of the BNC.

A state of C*c*O with the same optical characteristics as $\mathbf{P_M}$ can be generated by forcing the catalytic cycle backwards, starting from the ferric/cupric state **O** (Fig. 2). This was done in experiments with intact mitochondria, where oxidized C*c*O was exposed to a high pmf using ATP hydrolysis by reversal of the F_oF_1-ATPase, combined with a high redox potential at cytochrome *c* achieved artificially by an excess of ferricyanide [47,48]. Redox titrations of the $\mathbf{P_M}$ state [47] formed this way showed that it is the product of a two-electron oxidation of the ferric/cupric BNC plus water, which is why the name **P** (for peroxy) was given. However, work by Weng and Baker [49], Kitagawa and Ogura [42] and Fabian et al. [50] convincingly showed that the O—O bond is broken in the $\mathbf{P_M}$ state, a reaction that requires 4 electrons transferred to O_2. It was proposed that the heme a_3 Fe is in a hypervalent ferryl state, Fe(IV) = O^{2-} [51]. The electronic structure of the BNC in the $\mathbf{P_M}$ state has been confirmed spectroscopically [52] to contain ferryl Fe[IV] = O^{2-}, Cu(II), and a neutral crosslinked tyrosyl radical shown in (**2**).

2. Fe[IV] = O^{2-} $^-$HO-Cu[II]
   His-Tyr-O*

The formation of the $\mathbf{P_M}$ state from the mixed valence state of the enzyme plus O_2 involves the transfer of 4 electrons to the O_2. Two electrons are derived from the heme a_3 Fe(II) → Fe(IV), one from Cu_B(I) → Cu_B(II), and one from the crosslinked His-Tyr-OH → His-Tyr-O$^\bullet$ [50], which is also the source of the proton required in the O—O bond splitting reaction [53]. Another way to consider this reaction is that two of the four electrons transferred to O_2 correspond to the reducing equivalents used to reduce the BNC to the heme a_3 Fe(II)/Cu_B(I), the "third" electron comes from forming the hypervalent heme a_3 Fe(IV) state and the "fourth" electron comes from the crosslinked tyrosine.

Recently, based on cryoEM data, Michel et al. [54] proposed a ferric/cupric structure for the $\mathbf{P_M}$ state with a bound dioxygen molecule, or alternatively, a bound peroxide as had been suggested originally [47], but which was subsequently disproved [50,52], as discussed above. Fabian et al. [50], Jose et al. [52] and Michel et al. [54] all produced the $\mathbf{P_M}$ state by treating the oxidized enzyme with CO and O_2, a method originally introduced by Nicholls and Chanady [55]. This method is based on the water-gas shift reaction

$$\mathrm{CO + H_2O \rightarrow CO_2 + 2e^- + 2H^+}$$

where CO donates two reducing equivalents to the binuclear site, itself being oxidized to CO_2. The resulting mixed valence (**MV**) enzyme subsequently reacts with the provided O_2 to produce state $\mathbf{P_M}$. It was suggested in [54] that the evidence of a split O—O bond in $\mathbf{P_M}$ from the $H_2^{18}O$ yield after reaction of $^{18}O_2$ with **MV** C*c*O [50] could have arisen from a reaction between CO and O_2 to yield CO_2 and water. However, the direct uncatalysed reaction between CO and O_2 is negligible at room temperatures [56].

A further serious concern regarding the cryoEM interpretation of the $\mathbf{P_M}$ structure [54] arises from the fact that the optical spectrum of the enzyme suggested to be in that state shows only a very small absorption

at its characteristic peak at 607 nm and almost no signature of its 430 nm Soret band [54]. Hence, the state described as P_{CO} in ref. [54] could not possibly contain >10 % of state **P_M** and must be a heterogeneous mixture of forms.

Whereas the reaction of O_2 with the 2-electron reduced **MV** state of C*c*O produced the **P_M** state, not surprisingly, the reaction of the 4-electron reduced **FR** state of C*c*O with O_2 proceeds differently. Compound **A** (**1**) is again formed initially, followed by a state with optical characteristics identical to **P_M** [57] However, in this case the "fourth" electron does not come from the His-Tyr cofactor but from the low spin heme *a*: heme *a* Fe[II] → heme *a* Fe[III]. The proton is still donated by the crosslinked His-Tyr-OH, forming a tyrosinate His-Tyr-O^- [53]. This is called the **P_R** state (**3**) as it derives from the fully reduced (**FR**) enzyme. EPR studies [57,58] strongly suggest that the O—O bond is broken in the **P_R** state of C*c*O, as it is in the **P_M** state, and that Cu_B(II) is ligated to a hydroxide anion (OH^-) the oxygen atom of which derives from O_2.

The structure of the **P_R** state is, therefore,

3. Fe[IV] = O^{2-} $^-$HO-Cu[II]
   His-Tyr-O^-

also supported by a recent time-resolved serial femtosecond crystallography study [59]. The unusual EPR signal of copper in this state is successfully modelled as due to weak magnetic coupling between the ferryl heme a_3 Fe[IV] = O^{2-} (S = 1) and Cu_B [II] (S = 1/2), [57]. The P_R state is unique among the identified catalytic intermediates (as indicated by the dashed rectangle in Fig. 2). It is the only known intermediate separating the electron transfer to the BNC from the 'chemical' proton uptake to form the equivalent of water. Consequently, it is also the only intermediate with an apparent extra negative charge, which presumably reflects an intermediate state of the proton pumping process in which a proton-loading site is occupied that compensates for the charge imbalance (see [57]; dashed red arrows in Fig. 2).

5. The F state

The **F** state is observed as an intermediate following the appearance of the **P_R** state in the rapid kinetics of the reaction of O_2 with the fully reduced **FR** state using the flow/flash technique [60]. This **F** state is also observed in intact mitochondria by ATP-linked partial reversal of the catalytic cycle already described for state **P_M**, but in this case redox titrations revealed that state **F** is formed by a one-electron oxidation of state **O** [47].

The **F** state of the BNC has the same number of electrons as state **P_R** and is distinguished from the latter by an additional proton within the BNC, known to be taken up on the transition from state **P_R** to state **F** in the forward reaction. FTIR experiments showed that the anionic tyrosine remains unprotonated in state **F** [61], so protonation of the hydroxy-ligand of Cu_B seems likely and is supported by quantum chemical energy calculations. Such calculations also suggest that the water molecule produced dissociates away from the copper [62,63]. The basic structure of state **F** may therefore be written as

4. Fe[IV] = O^{2-} Cu[II]
   His-Tyr-O^-

However, density functional QM calculations further suggest the presence of considerable spin on the tyrosine [62,64] indicating that the true structure is likely to differ from the above by shifting an electron from the tyrosinate to Cu[II] to form the tyrosyl free radical, as below.

5. Fe[IV] = O^{2-} Cu[I]
   His-Tyr-O*

or an equilibrium mix of the two structures **4** and **5**.

6. The enigmatic O states

When mammalian cytochrome *c* oxidase is extracted and purified, this 'as isolated' form is classically described as 'fully oxidized', generally called state **O**, with all four metal centers in their ferric/cupric states. However, considerable variations and heterogeneity in the state of the BNC can exist, depending on the methodology of the isolation procedure. One type of heterogeneity arises from ligands that can bind to the BNC during purification. These include halides and bicarbonate and the experimental distinction between them and the unligated **O** state can be subtle [65]. A second type of heterogeneity can arise from the relaxation of the unligated **O** state into a form termed 'slow' that reacts very slowly with added BNC ligands and in which electron transfer into the BNC is hindered [66]. This form is favoured when isolated C*c*O is incubated at low pH and displays a very distinctive blueshift of its heme a_3 Soret peak from 424 to 414 nm, like that induced by binding of formate to the BNC. To date, the chemical nature of this form remains obscure, with possibilities being an internal protonic rearrangement or even formation of a true peroxide state. The presence of these altered forms of isolated C*c*O have not always been appreciated, with the term 'resting' being applied to different forms, or mixtures of forms, of isolated, oxidized C*c*O, making some earlier published data difficult to interpret. However, the ligated and 'slow' forms of **O** can be converted into the unligated 'pulsed/fast' **O** state by a pulsing cycle of reduction/reoxidation [66].

In 2004 Bloch et al. [67] demonstrated that oxidation of the fully reduced enzyme initially leads to a metastable, additional **O** state that subsequently relaxes to the more stable 'pulsed/fast' **O** state within a few seconds. Energy transduction (including proton pumping) proceeds upon further reduction only from the metastable form of the **O** state (see also [68]). At about the same time, Rousseau et al. [69] showed by time-resolved Raman spectroscopy of the forward reaction that the decay of the **F** state transiently yielded a state best described as an unusual high spin ferric hydroxide species. This form decayed to the final (presumably 'pulsed/fast') **O** state in some 5 ms. However, this is a minimum lifetime since the measured decay may have been caused by exchange of the ^{18}O-labelled OH^- ligand. It thus seems very likely that the metastable form of state **O** is identical to Rousseau's ferric hydroxide species, which is why it has been named state **O_H**, as opposed to the more stable 'pulsed/fast' **O** form.

Density functional analyses by Sharma et al. [70] suggested that the **O_H** state may have the following structure, obtained by adding one electron and one proton to the **F** state

6. Fe[III]-OH^-… Cu[II]
   His-Tyr-O^-

i.e., a high spin ferric heme species with a distal hydroxide ligand bridging between the two metals. This has been supported by the quantum-chemical calculations of Blomberg and Siegbahn [71] and Noodleman et al. [63]. It is noteworthy that it is very unusual that a ferric heme with the strong-field hydroxide ligand would still be high spin. However, here this is attributed to the bridging of the OH^- iron ligand to the copper (or possibly to a water molecule). As was the case with the modeling of the **F** state, considerable spin at the tyrosine suggests the following alternative structure of the **O_H** state

7. Fe[III]-OH^-… Cu[I]
   His-Tyr-O*

in equilibrium with the former structure (**6**).

One further complication on the structure of a highly purified 'as prepared' **O** state preparation was the finding that 6 electron equivalents were required to fully reduced it with added dithionite. This led to a proposal that the **O** state contains a peroxide ligand [72]. However, reduction with NADH/PMS required only 4 electron equivalents,

consistent with other literature reports e.g. [73]. In addition, the enzyme used in [72] was stated to be in a 'resting' form, which raises the question of whether this might represent the non-catalytic 'slow' form, which could be an inactive peroxide-containing **O** state. Several X-ray studies [7,74–76], and a recent cryoEM study [54], have also been interpreted to suggest that the (presumably pulsed/fast) **O** state has a peroxide bound in the BNC. However, such a possibility is contradicted by computational findings that a peroxide adduct would not be a stable species [63]. In fact, it is well known from spectroscopic studies that adding peroxide to the pulsed/fast **O** results in the formation of the $\mathbf{P_M}$ and/or **F** states, depending on concentration and pH (cf. above).

Noodleman et al. [63] have made the interesting proposal that the 'peroxide observed in structural studies of C*c*O in the **O** state' is an experimental artefact arising from a heterogeneous mixture of forms. In their view it is due to an overlap of positions of a water molecule between the heme iron and the copper in the BNC. Hence, the relaxed (pulsed/fast) **O** state may have the structure

8. Fe[III]—OH_2–Cu[II]
   His-Tyr-O^-

This structure, and the absence of a peroxide, is reminiscent of the structure reported by Andersson et al. [77] for the oxidized state of CcO of cytochrome ba_3 from *Thermus thermophilus* by serial femtosecond crystallography at room temperature using an X-ray free electron laser.

Note that this state (**8**) has an additional proton in the BNC as compared with (**6**) and (**7**). Blomberg and Siegbahn [71] have also suggested that the pulsed/fast **O** state is a protonated form of state $\mathbf{O_H}$, but has assigned the proton to the tyrosine, i.e.

9. Fe[III]—OH^-…Cu[II]
   His-Tyr-OH

An extra proton in pulsed/fast state **O**, as in BNC structures (**8**) and (**9**), compared to state $\mathbf{O_H}$, would mean that it had a difference of three protons compared to the structure of the reduced BNC in the **FR** state and that two protons are required for its formation from **F** (structures **4** and **5** above). However, the transition of **F** to the pulsed/fast **O** state is accompanied by net uptake of only one proton from the external medium [78]. In addition, at least in bovine and *R. sphaeroides* C*c*O, the transition from the **FR** or **MV** state into pulsed/fast **O** is linked to a two proton change of the BNC in both the forward [79,80] and reverse [81] directions, though a larger (2.5 ± 0.6 H^+) change has been reported for the BNC of *Paracoccus* C*c*O [82]. Overall, these data strongly support a difference within the BNC of two protons between pulsed/fast **O** and **FR** states, as is the case for the transition between the predicted structure of $\mathbf{O_H}$ and the reduced **R** state BNC in Fig. 2. Hence, if there is indeed an extra proton in 'pulsed/fast' **O**, which has yet to be confirmed experimentally, it would have to arise reversibly from an internal site [83,84]. The conserved lysine-319 (bovine C*c*O subunit I numbering) in the proton-conducting K-channel is an interesting candidate as electrostatic calculations showed it to be highly protonated in the **R** state [85]. The positive charge of lysine-319, which has been shown in MD simulations to flip upwards towards the BNC (and see ref. [53]), may be required to raise the redox potential of the BNC in the $\mathbf{O_H}$ state to ascertain fast electron transfer and a sufficient driving force for proton translocation [33,83]. Such a scenario would readily explain why the analogue of the lysine-319-methionine variant of the *P. denitrificans* enzyme behaves as if it were in the **O** state rather than $\mathbf{O_H}$, and unable to catalyse fast electron transfer and proton translocation [67].

One may tentatively suggest that the **O** state (i.e., the pulsed/fast **O**) may have a structure very similar to the metastable $\mathbf{O_H}$ state, but with an additional proton at the bridging ligand derived internally from the lysine in the K-channel (structure **8**). We may also speculate that in the classical slow form of the enzyme, known to be favoured at low pH, an external proton has protonated the tyrosine of the BNC (structure **9**) leading to a blockade of reduction of the BNC. Finally, it should be remembered that water molecules are produced at the BNC by turnover. These water molecules may be required for the fast proton-coupled electron transfer reactions characteristic of catalysis [27]. Cessation of turnover may thus dry out the surroundings of the BNC, and lead to the decay of a catalytically active metastable state $\mathbf{O_H}$ to a more stable dry state **O**.

All in all, it is somewhat paradoxical that the forms of the enzyme as isolated (state **O**) may be the least understood. One contributing aspect may well be that this state can be heterogeneous, a fact that has not always been recognized as noted above. Another aspect of this that might be of importance in future research is that the relaxation from state $\mathbf{O_H}$ to other forms of **O** might be of physiological importance and involved in regulating the energy-transducing efficiency of mammalian cytochrome *c* oxidase.

7. Re-reduction of the binuclear centre

Time-resolved single electron injection into cytochrome oxidase in the $\mathbf{O_H}$ state [28] resulted in a blue shift of the near infrared band at 655 nm, but no indication (<1 %) of reduction of heme a_3. The absorption band near 655 nm is considered to be due to charge transfer between ferric heme a_3 and Cu_B[II], so its shift to the blue in these experiments most likely reflects reduction of Cu_B to the cuprous form. Alternatively, and in agreement with [86] this event could be envisaged as a reduction of the neutral tyrosine radical in structure (**7**), which is thought to equilibrate with the structure (**6**) in the state we have called $\mathbf{O_H}$. In either case, the structure of the next intermediate, $\mathbf{E_H}$, would be (**10**), or (**11**), obtained by adding one electron and a proton to state $\mathbf{O_H}$, either (**6**) or (**7**). These proposed structures of $\mathbf{E_H}$ are supported by recent X-ray-determined structures of catalytic intermediates of bovine C*c*O [87].

10. Fe[III]-OH^-… Cu[I]
    His-Tyr-OH
11. Fe[III]-OH_2… Cu[I]
    His-Tyr-O^-

Margareta Blomberg proposed on the basis of density functional calculations that Cu_B may already be reduced in state $\mathbf{O_H}$ and that the transition to state $\mathbf{E_H}$ in part involves reduction of heme a_3 and in part reduction of the tyrosine radical (ref. [86]; Table 2). In our view the experimental data [28] exclude significant reduction of heme a_3 in the $\mathbf{E_H}$ state (cf. above).

8. Free energy changes

Table 1 summarizes the individual standard free energy changes of all individual reaction steps of the catalytic cycle, assuming a redox midpoint potential ($E_{m,7}$) of 0.25 V (versus NHE) for the electron donor, cytochrome *c*, and estimates of the $E_{m,7}$ values of the individual redox couples based either on experimental titrations (see [30]) or on the most recent DFT calculations by Blomberg [86]. It is worth noting that the sum of free energies of all reaction steps must match the known overall standard free energy change of reducing O_2 to 2 H_2O by four molecules of ferrocytochrome *c* (2.2 eV). It should also be noted that two partial reactions in the cycle, the binding of O_2 ($\mathbf{R} \rightarrow \mathbf{A}$) and the $\mathbf{A} \rightarrow \mathbf{P_M}$ step, are not linked to reduction of the BNC by cytochrome c_{red}. The free energy change upon O_2 binding to the BNC is close to zero as indicated by the high dissociation constant [35–37]. The free energy change for the $\mathbf{A} \rightarrow \mathbf{P_M}$ step has been estimated to be between ca. -3.5 kcal/mol (−0.15 eV) [30] and ca. -7 kcal/mol (−0.30 eV) [86] based on quantum-chemical calculations. All other free energy changes and redox potentials are based on experimental data [30], or on corresponding results from most recent DFT calculations [86]. The experimental data concerning the $\mathbf{O_H} \rightarrow \mathbf{E_H}$ step originally stem from ref. [28] where it was found that one-electron reduction of $\mathbf{O_H}$ resulted exclusively in reduction of Cu_B. The

Table 1
Energies and midpoint redox potentials for the transitions in the catalytic cycle.

Transition	Midpoint redox potential ($E_{m,7}$; mV)		Reaction energy ($-\Delta G_0'$; meV)	
	Experimental	Computational [86]	Experimental	Computational [86]
R → **A**	–	–	20[a]	20
A → $\mathbf{P_M}$	–	–	300[a]	300
$\mathbf{P_M}$ → **F**	860	1050	610	800
F → $\mathbf{O_H}$	800	680	550	430
$\mathbf{O_H}$ → $\mathbf{E_H}$	>520[b]	650	>270[b]	400
$\mathbf{E_H}$ → **R**	<700[c]	500	<450[c]	250
Sum	2880	2880	2200	2200

All the experimental data, except the reaction energy for the **A** → $\mathbf{P_M}$ transition, are based on results from redox titrations in mitochondria (see [30]), and time-resolved electron injection experiments [28]. The redox potentials are $E_{m,7}$ values relative to the NHE. Reaction energies (except for **A** → $\mathbf{P_M}$ and **R** → **A**) are based on the difference between the relevant $E_{m,7}$ of the transition and the $E_{m,7}$ of the electron donor, cytochrome *c*, taken as 250 mV. The redox potential of the O_2/H_2O couple is taken as 800 mV (per electron), i.e. 3200 mV for the four electron reaction. Since the true standard redox potential is 815 mV (for an O_2 concentration of 1 *m*) at pH = 7, the applied 800 mV corresponds to a more experimentally relevant O_2 concentration of ca. 120 μM. The total energy of the reaction must equal the total energy of O_2 reduction by ferrocytochrome *c*, thus (800–250) meV x4 = 2200 meV. The computational data are based on the most recent DFT calculations by Blomberg [86], using the values in her Table 2.

[a] These values are not experimental but are predictions from simulations in [86].

[b] The experimentally assessed lower limit for the $E_{m,7}$ [28] (see text), and the corresponding free energy.

[c] The maximum $E_{m,7}$ and free energy are based on the known sum of all free energy values.

$E_{m,7}$ was estimated to be at least 100 mV higher than the $E_{m,7}$ of heme *a* [28], which is ca. 400 mV in cytochrome oxidase from *Paracoccus denitrificans* [88]. Since we have subsequently estimated that 1 % reduction of the heme groups would have been distinguished in the work described in [28], we have set the lower limit for the $E_{m,7}$ of the $\mathbf{O_H}$ → $\mathbf{E_H}$ reaction to 400 + 120 = 520 mV in Table 1.

Kruse et al. [89] recently reported on a resonance Raman band at 750 cm^{-1} specific for the pulsed/fast **O** state, but absent in the slow **O**, which titrated with an $E_{m,8}$ of ca. 525 mV relative to the Ag/AgCl electrode and was suggested to correspond to the tyrosine radical. This redox potential is equal to ca. 755 mV versus the NHE assuming a standard Ag/AgCl reference electrode was used, and we suggest that the authors were driving the **O** (pulsed/fast) state back to state **F** (states **4** and **5** above; see also Fig. 2). With the known 1 H^+/e^- dependence of that reaction, the corresponding $E_{m,7}$ would be 815 mV (vs. NHE), in excellent agreement with earlier experiments with intact mitochondria (Table 1). The authors interpreted the absence of this Raman feature in the slow **O** state by protonation of the tyrosine, which agrees with our conclusions above.

Comparison of the experimental and computational estimates in Table 1 shows a reasonably good fit considering the uncertainties involved in both methodologies. However, in the reductive phase the $\mathbf{E_H}$ → **R** transition in particular is predicted to have a standard free energy change (Table 1) hardly sufficient to drive two electrical charges across the membrane with a protonmotive force of some 200 mV. Yet, the low computational $E_{m,7}$ value for the $\mathbf{E_H}$ → **R** transition need not be a problem. All values given are based on standard states (midpoint potentials, $E_{m,7}$). However, the *ambient* redox potential of the $\mathbf{E_H}$/**R** redox couple during catalytic turnover may be much higher than the one deduced from the $E_{m,7}$ value because we would expect the occupancy of state $\mathbf{E_H}$ to be much higher than that of state **R** in the aerobic steady state. One should also keep in mind that the proton-pumping efficiency of cytochrome ***c*** oxidase [90] is ca. 80 % at a protonmotive force of 170 mV, and likely to be much lower at 200 mV. Hence, the latter value may be too high as a norm in assessing the required free energy of individual steps of the catalytic cycle.

Despite of the above, it is clear that the experimental $E_{m,7}$ values for re-reduction of the BNC starting from the pulsed/fast state **O** (as opposed to the metastable $\mathbf{O_H}$), as obtained in anaerobic redox titrations (i.e. ca. 400 mV at most for **O** → **E** and **E** → **R**) are far too low to be consistent with the requirement that the sum of all free energies in the catalytic cycle must equal the free energy of O_2 reduction to water (see above). In our view this means that the energy of the pulsed/fast **O** state must be lower than that of the metastable $\mathbf{O_H}$ state to an extent that compensates for the low $E_{m,7}$ values. Density functional analyses of possible pulsed/fast **O** states have not yielded lower energies than that of state $\mathbf{O_H}$ [84], so this is a remaining dilemma. However, we find it possible that a drying up of the hydrophobic cavity next to the BNC on cessation of activity may contribute to lowering the energy.

9. Epilogue

The catalytic cycle of CcO involves the transfer of four electrons and four protons onto dioxygen to produce two H_2O products. Since these are supplied in single steps, the number of catalytic intermediates is inevitably large, with some stable enough to study with biophysical methods and others too transient to trap. Even for those stable enough to study, complications arise from multiple forms that can exist. This is particularly evident for the fully oxidized **O** state which, besides being able to form a range of stable states, appears to have a relatively unstable form when the enzyme is cycling through its natural proton-pumping cycle. The structures of these enigmatic forms of the **O** state are still not fully resolved, prompting ongoing controversy on the structures of it and other catalytic intermediates of the natural catalytic cycle. In this review, we have attempted to summarize their most likely structures, based on currently available biophysical data. Knowing the correct structures of these intermediates is essential when linking them to the coupled proton translocations that accompany their interconversions, a topic beyond the scope of the present article.

Declaration of competing interest

The authors declare that they have no known competing financial interests or personal relationships that could have appeared to influence the work reported in this paper.

Data availability

No data was used for the research described in the article.

References

[1] V.R.I. Kaila, M. Wikstrom, Architecture of bacterial respiratory chains, Nat. Rev. Microbiol. 19 (2021) 319–330.
[2] T. Tsukihara, H. Aoyama, E. Yamashita, T. Tomizaki, H. Yamaguchi, K. Shinzawa-Itoh, R. Nakashima, R. Yaono, S. Yoshikawa, The whole structure of the 13-subunit oxidized cytochrome c oxidase at 2.8 A, Science 272 (1996) 1136–1144.
[3] S. Iwata, C. Ostermeier, B. Ludwig, H. Michel, Structure at 2.8 a resolution of cytochrome c oxidase from paracoccus denitrificans, Nature 376 (1995) 660–669.
[4] S. Buschmann, E. Warkentin, H. Xie, J.D. Langer, U. Ermler, H. Michel, The structure of cbb3 cytochrome oxidase provides insights into proton pumping, Science 329 (2010) 327–330.
[5] L. Qin, C. Hiser, A. Mulichak, R.M. Garavito, S. Ferguson-Miller, Identification of conserved lipid/detergent-binding sites in a high-resolution structure of the membrane protein cytochrome c oxidase, Proc. Natl. Acad. Sci. U. S. A. 103 (2006) 16117–16122.
[6] T. Soulimane, G. Buse, G.P. Bourenkov, H.D. Bartunik, R. Huber, M.E. Than, Structure and mechanism of the aberrant ba3-cytochrome c oxidase from Thermus thermophilus, EMBO J. 19 (2000) 1766–1776.
[7] T. Tiefenbrunn, W. Liu, Y. Chen, V. Katritch, C.D. Stout, J.A. Fee, V. Cherezov, High resolution structure of the ba3 cytochrome c oxidase from thermus thermophilus in a lipidic environment, PLoS One 6 (2011), e22348.
[8] J. Xu, Z. Ding, B. Liu, S.M. Yi, J. Li, Z. Zhang, Y. Liu, L. Liu, A. Zhou, R.B. Gennis, J. Zhu, Structure of the cytochrome aa 3–600 heme-copper menaquinol oxidase

bound to inhibitor HQNO shows TM0 is part of the quinol binding site, Proc. Natl. Acad. Sci. U. S. A. 117 (2019) 872–876.
[9] J. Li, L. Han, F. Vallese, Z. Ding, S.K. Choi, S. Hong, Y. Luo, B. Liu, C.K. Chan, E. Tajkhorshid, J. Zhu, O. Clarke, K. Zhang, R. Gennis, Cryo-EM structures of Escherichia coli cytochrome Bo 3 reveal bound phospholipids and ubiquinone-8 in a dynamic substrate binding site, Proc. Natl. Acad. Sci. U. S. A. 118 (2021).
[10] W. Wu, C.K. Chang, C. Varotsis, G.T. Babcock, A. Puustinen, M. Wikström, Structure of the heme o prosthetic group from the terminal quinol oxidase of Escherichia coli, J. Am. Chem. Soc. 114 (1992) 1182–1187.
[11] J. Hemp, D.E. Robinson, K.B. Ganesan, T.J. Martinez, N.L. Kelleher, R.B. Gennis, Evolutionary migration of a post-translationally modified active-site residue in the proton-pumping heme-copper oxygen reductases, Biochemistry 45 (2006) 15405–15410.
[12] V. Rauhamaki, M. Baumann, R. Soliymani, A. Puustinen, M. Wikstrom, Identification of a histidine-tyrosine cross-link in the active site of the cbb3-type cytochrome c oxidase from rhodobacter sphaeroides, Proc. Natl. Acad. Sci. U. S. A. 103 (2006) 16135–16140.
[13] F.L. Sousa, R.J. Alves, M.A. Ribeiro, J.B. Pereira-Leal, M. Teixeira, M.M. Pereira, The superfamily of heme–copper oxygen reductases: types and evolutionary considerations, Biochim. Biophys. Acta Biomembr. 2012 (1817) 629–637.
[14] M.M. Pereira, M. Santana, M. Teixeira, A novel scenario for the evoluation of haem-copper oxygen reductases, Biochim. Biophys. Acta 1505 (2001) 185–208.
[15] R. Murali, J. Hemp, R.B. Gennis, Evolution of quinol oxidation within the heme-copper oxidoreductase superfamily, Biochim. Biophys. Acta Bioenergetics 1863 (2022), 148907.
[16] S. Yoshikawa, K. Shinzawa-Itoh, T. Tsukihara, Crystal structure of bovine heart cytochrome c oxidase at 2.8 Å resolution, J. Bioenerg. Biomemb. 30 (1998) 7-.
[17] K. Shinzawa-Itoh, T. Sugimura, T. Misaki, Y. Tadehara, S. Yamamoto, M. Hanada, N. Yano, T. Nakagawa, S. Uene, T. Yamada, H. Aoyama, E. Yamashita, T. Tsukihara, S. Yoshikawa, K. Muramoto, Monomeric structure of an active form of bovine cytochrome c oxidase, Proc. Natl. Acad. Sci. U. S. A. 116 (2019) 19945–19951.
[18] J.M. Di Trani, A. Moe, D. Riepl, P. Saura, V.R.I. Kaila, P. Brzezinski, J.L. Rubinstein, Structural basis of mammalian complex IV inhibition by steroids, Proc. Natl. Acad. Sci. U. S. A. 119 (2022), e2205228119.
[19] C. Ostermeier, A. Harrenga, U. Ermler, H. Michel, Structure at 2.7 Å resolution of the paracoccus denitrificans two-subunit cytochrome c oxidase complexed with an antibody Fv fragment, Proc. Natl. Acad. Sci. U. S. A. 94 (1997) 10547–10553.
[20] L. Qin, J. Liu, D.A. Mills, D.A. Proshlyakov, C. Hiser, S. Ferguson-Miller, Redox-dependent conformational changes in cytochrome C oxidase suggest a gating mechanism for proton uptake, Biochemistry 48 (2009) 5121–5130.
[21] J. Abramson, S. Riistama, G. Larsson, A. Jasaitis, M. Svensson-Ek, L. Laakkonen, A. Puustinen, S. Iwata, M. Wikstrom, The structure of the ubiquinol oxidase from Escherichia coli and its ubiquinone binding site, Nat. Struct. Biol. 7 (2000) 910–917.
[22] J. Gu, M. Wu, R. Guo, K. Yan, J. Lei, N. Gao, M. Yang, The architecture of the mammalian respirasome, Nature 537 (2016) 639–643.
[23] R. Guo, S. Zong, M. Wu, J. Gu, M. Yang, Architecture of human mitochondrial respiratory megacomplex I2III2IV2, Cell 170 (2017) 1247–1257 e1212.
[24] J.A. Letts, L.A. Sazanov, Clarifying the supercomplex: the higher-order organization of the mitochondrial electron transport chain, Nat. Struct. Mol. Biol. 24 (2017) 800–808.
[25] A.M. Hartley, N. Lukoyanova, Y. Zhang, A. Cabrera-Orefice, S. Arnold, B. Meunier, N. Pinotsis, A. Marechal, Structure of yeast cytochrome c oxidase in a supercomplex with cytochrome bc1, Nat. Struct. Mol. Biol. 26 (2019) 78–83.
[26] S. Rathore, J. Berndtsson, L. Marin-Buera, J. Conrad, M. Carroni, P. Brzezinski, M. Ott, Cryo-EM structure of the yeast respiratory supercomplex, Nat. Struct. Mol. Biol. 26 (2019) 50–57.
[27] M. Maldonado, F. Guo, J.A. Letts, Atomic structures of respiratory complex III2, complex IV, and supercomplex III2-IV from vascular plants, elife 10 (2021).
[28] I. Belevich, D.A. Bloch, N. Belevich, M. Wikstrom, M.I. Verkhovsky, Exploring the proton pump mechanism of cytochrome c oxidase in real time, Proc. Natl. Acad. Sci. U. S. A. 104 (2007) 2685–2690.
[29] M. Wikstrom, M.I. Verkhovsky, Towards the mechanism of proton pumping by the haem-copper oxidases, Biochim. Biophys. Acta 1757 (2006) 1047–1051.
[30] M. Wikstrom, K. Krab, V. Sharma, Oxygen activation and energy conservation by cytochrome c oxidase, Chem. Rev. 118 (2018) 2469–2490.
[31] M. Wikstrom, V. Sharma, V.R. Kaila, J.P. Hosler, G. Hummer, New perspectives on proton pumping in cellular respiration, Chem. Rev. 115 (2015) 2196–2221.
[32] P. Brzezinski, R.B. Gennis, Cytochrome c oxidase: exciting progress and remaining mysteries, J. Bioenerg. Biomembr. 40 (2008) 521–531.
[33] P.R. Rich, Mitochondrial cytochrome c oxidase: catalysis, coupling and controversies, Biochem. Soc. Trans. 45 (2017) 813–829.
[34] S. Yoshikawa, A. Shimada, Reaction mechanism of cytochrome c oxidase, Chem. Rev. 115 (2015) 1936–1989.
[35] B. Chance, C. Saronio, J.S. Leigh Jr., Functional intermediates in the reaction of membrane-bound cytochrome oxidase with oxygen, J. Biol. Chem. 250 (1975) 9226–9237.
[36] M.I. Verkhovsky, J.E. Morgan, A. Puustinen, M. Wikström, Kinetic trapping of oxygen in cell respiration, Nature 380 (1996) 268–270.
[37] M.I. Verkhovsky, J.E. Morgan, M. Wikström, Oxygen binding and activation: early steps in the reaction of oxygen with cytochrome c oxidase, Biochemistry 33 (1994) 3079–3086.
[38] K. Krab, H. Kempe, M. Wikstrom, Explaining the enigmatic K(M) for oxygen in cytochrome c oxidase: a kinetic model, Biochim. Biophys. Acta 2011 (1807) 348–358.
[39] M. Kaukonen, Calculated reaction cycle of cytochrome c oxidase, J. Phys. Chem. B 111 (2007) 12543–12550.
[40] M.R.A. Blomberg, P.E.M. Siegbahn, G.T. Babcock, M. Wikström, Modeling cytochrome oxidase: a quantum chemical study of the O−O bond cleavage mechanism, J. Am. Chem. Soc. 122 (2000) 12848–12858.
[41] S. Han, Y.-C. Ching, D.L. Rousseau, Primary intermediate in the reaction of oxygen with fully reduced cytochrome c oxidase, Proc. Natl. Acad. Sci. U. S. A. 87 (1990) 2491–2495.
[42] T. Kitagawa, T. Ogura, Time-resolved resonance Raman investigation of oxygen reduction mechanism of bovine cytochrome c oxidase, J. Bioenerg. Biomembr. 30 (1998) 71-.
[43] C. Weber, D.J. Cole, D.D. O'Regan, M.C. Payne, Renormalization of myoglobin-ligand binding energetics by quantum many-body effects, Proc. Natl. Acad. Sci. U. S. A. 111 (2014) 5790–5795.
[44] K. Shikama, Nature of the FeO2 bonding in myoglobin and hemoglobin: a new molecular paradigm, Prog. Biophys. Mol. Biol. 91 (2006) 83–162.
[45] M.I. Verkhovsky, J.E. Morgan, M. Wikström, Redox transitions between oxygen intermediates in cytochrome-c oxidase, Proc. Natl. Acad. Sci. U. S. A. 93 (1996) 12235–12239.
[46] F. Poiana, C. von Ballmoos, N. Gonska, M.R.A. Blomberg, P. Ädelroth, P. Brzezinski, Splitting of the O-O bond at the heme-copper catalytic site of respiratory oxidases, Sci. Adv. 3 (2017), e1700279.
[47] M. Wikström, Identification of the electron transfers in cytochrome oxidase that are coupled to proton-pumping, Nature 338 (1989) 776–778.
[48] J.E. Morgan, M. Wikström, Steady-state redox behavior of cytochrome c, cytochrome a, and CuA of cytochrome c oxidase in intact rat liver mitochondria, Biochemist 30 (1991) 948–958.
[49] L. Weng, G.M. Baker, Reaction of hydrogen peroxide with the rapid form of resting cytochrome oxidase, Biochemist 30 (1991) 5727–5733.
[50] M. Fabian, W.W. Wong, R.B. Gennis, G. Palmer, Mass spectrometric determination of dioxygen bond splitting in the "peroxy" intermediate of cytochrome c oxidase, Proc. Natl. Acad. Sci. U. S. A. 96 (1999) 13114–13117.
[51] P. George, D.H. Irvine, A kinetic study of the reaction between ferrimyoglobin and hydrogen peroxide, J. Colloid Sci. 11 (1956) 327–339.
[52] A. Jose, A.W. Schaefer, A.C. Roveda Jr., W.J. Transue, S.K. Choi, Z. Ding, R. B. Gennis, E.I. Solomon, The three-spin intermediate at the O-O cleavage and proton-pumping junction in heme-Cu oxidases, Science 373 (2021) 1225–1229.
[53] E.A. Gorbikova, I. Belevich, M. Wikstrom, M.I. Verkhovsky, The proton donor for O O bond scission by cytochrome c oxidase, Proceedings of the National Academy of Sciences 105 (2008) 10733–10737.
[54] F. Kolbe, S. Safarian, Z. Piorek, S. Welsch, H. Muller, H. Michel, Cryo-EM structures of intermediates suggest an alternative catalytic reaction cycle for cytochrome c oxidase, Nat. Commun. 12 (2021) 6903.
[55] P. Nicholls, G.A. Chanady, Interactions of cytochrome aa3 with oxygen and carbon monoxide, Biochim. Biophys. Acta 634 (1981) 256–265.
[56] W.T. Rawlins, W.C. Gardiner, Rate constant for carbon monoxide + molecular oxygen = carbon dioxide + atomic oxygen from 1500 to 2500.Deg. K. Reevaluation of induction times in the shock-initiated combustion of hydrogen-oxygen-carbon monoxide-argon mixtures, J. Phys. Chem. 78 (1974) 497–500.
[57] J.E. Morgan, M.I. Verkhovsky, G. Palmer, M. Wikström, Role of the PR intermediate in the reaction of cytochrome c oxidase with O2, Biochemistry 40 (2001) 6882–6892.
[58] O. Hansson, B. Karlsson, R. Aasa, T. Vanngard, B.G. Malmstrom, The structure of the paramagnetic oxygen intermediate in the cytochrome c oxidase reaction, EMBO J. 1 (1982) 1295–1297.
[59] I. Ishigami, A. Lewis-Ballester, A. Echelmeier, G. Brehm, N.A. Zatsepin, T.D. Grant, J.D. Coe, S. Lisova, G. Nelson, S. Zhang, Z.F. Dobson, S. Boutet, R.G. Sierra, A. Batyuk, P. Fromme, R. Fromme, J.C.H. Spence, A. Ros, S.R. Yeh, D.L. Rousseau, Snapshot of an oxygen intermediate in the catalytic reaction of cytochrome c oxidase, Proc. Natl. Acad. Sci. U. S. A. 116 (2019) 3572–3577.
[60] J.E. Morgan, M.I. Verkhovsky, M. Wikström, Observation and assignment of peroxy and ferryl intermediates in the reduction of dioxygen to water by cytochrome c oxidase, Biochemistry 35 (1996) 12235–12240.
[61] E.A. Gorbikova, M. Wikstrom, M.I. Verkhovsky, The protonation state of the cross-linked tyrosine during the catalytic cycle of cytochrome c oxidase, J. Biol. Chem. 283 (2008) 34907–34912.
[62] V. Sharma, G. Enkavi, I. Vattulainen, T. Rog, M. Wikstrom, Proton-coupled electron transfer and the role of water molecules in proton pumping by cytochrome c oxidase, Proc. Natl. Acad. Sci. U. S. A. 112 (2015) 2040–2045.
[63] L. Noodleman, W.G. Han Du, D. McRee, Y. Chen, T. Goh, A.W. Götz, Coupled transport of electrons and protons in a bacterial cytochrome c oxidase-DFT calculated properties compared to structures and spectroscopies, Phys. Chem. Chem. Phys. 22 (2020) 26652–26668.
[64] M.R. Blomberg, Mechanism of oxygen reduction in cytochrome c oxidase and the role of the active site tyrosine, Biochemistry 55 (2016) 489–500.
[65] A.J. Moody, 'As prepared' forms of fully oxidised haem/Cu terminal oxidases, Biochim. Biophys. Acta 1276 (1996) 6–20.
[66] E. Antonini, M. Brunori, A. Colosimo, C. Greenwood, M.T. Wilson, Oxygen "Pulsed" cytochrome c oxidase: functional properties and catalytic relevance, Proc. Natl. Acad. Sci. U. S. A. 74 (1977) 3128–3132.
[67] D. Bloch, I. Belevich, A. Jasaitis, C. Ribacka, A. Puustinen, M.I. Verkhovsky, M. Wikström, The catalytic cycle of cytochrome c oxidase is not the sum of its two halves, PNAS 101 (2004) 529–533.
[68] M.I. Verkhovsky, A. Jasaitis, M.L. Verkhovskaya, J.E. Morgan, M. Wikström, Proton translocation by cytochrome c oxidasse, Nature 400 (1999) 480–483.

[69] S. Han, Y.-C. Ching, D.L. Rousseau, Ferryl and hydroxy intermediates in the reaction of oxygen with reduced cytochrome c oxidase, Nature 348 (1990) 89–90.
[70] V. Sharma, K.D. Karlin, M. Wikstrom, Computational study of the activated O(H) state in the catalytic mechanism of cytochrome c oxidase, Proc. Natl. Acad. Sci. U. S. A. 110 (2013) 16844–16849.
[71] M.R.A. Blomberg, P.E.M. Siegbahn, Protonation of the binuclear active site in cytochrome c oxidase decreases the reduction potential of CuB, biochimica et biophysica acta (BBA) -, Bioenergetics (2015, 1847) 1173–1180.
[72] M. Mochizuki, H. Aoyama, K. Shinzawa-Itho, T. Usui, T. Tsukihara, S. Yoshikawa, Quantitative reevaluation of the redox active sites of crystalline bovine heart cytochrome c oxidase, J. Biol. Chem. 274 (1999) 33403–33411.
[73] G.C.M. Steffens, T. Soulimane, G. Wolff, G. Buse, Stochiometry and redox behaviour of metals in cytochrome-c oxidase, Eur. J. Biochem. 213 (1993) 1149–1157.
[74] J. Koepke, E. Olkhova, H. Angerer, H. Muller, G. Peng, H. Michel, High resolution crystal structure of paracoccus denitrificans cytochrome c oxidase: new insights into the active site and the proton transfer pathways, Biochim. Biophys. Acta 1787 (2009) 635–645.
[75] G. Ueno, A. Shimada, E. Yamashita, K. Hasegawa, T. Kumasaka, K. Shinzawa-Itoh, S. Yoshikawa, T. Tsukihara, M. Yamamoto, Low-dose X-ray structure analysis of cytochrome c oxidase utilizing high-energy X-rays, J. Synchrotron Radiat. 26 (2019) 912–921.
[76] K. Hirata, K. Shinzawa-Itoh, N. Yano, S. Takemura, K. Kato, M. Hatanaka, K. Muramoto, T. Kawahara, T. Tsukihara, E. Yamashita, K. Tono, G. Ueno, T. Hikima, H. Murakami, Y. Inubushi, M. Yabashi, T. Ishikawa, M. Yamamoto, T. Ogura, H. Sugimoto, J.R. Shen, S. Yoshikawa, H. Ago, Determination of damage-free crystal structure of an X-ray-sensitive protein using an XFEL, Nat. Methods 11 (2014) 734–736.
[77] R. Andersson, C. Safari, R. Dods, E. Nango, R. Tanaka, A. Yamashita, T. Nakane, K. Tono, Y. Joti, P. Båth, E. Dunevall, R. Bosman, O. Nureki, S. Iwata, R. Neutze, G. Brändén, Serial femtosecond crystallography structure of cytochrome c oxidase at room temperature, Sci. Rep. 7 (2017) 4518.
[78] R. Mitchell, P. Mitchell, P.R. Rich, Protonation states of the catalytic intermediates of cytochrome c oxidase, Biochim. Biophys. Acta 1101 (1992) 188–191.
[79] P. Ädelroth, M. Ek, P. Brzezinski, Factors determining electron-transfer rates in cytochrome c oxidase: investigation of the oxygen reaction in the R. Sphaeroides enzymes, Biochim. Biophys. Acta (1998, 1367) 107–117.
[80] R. Mitchell, P.R. Rich, Proton uptake by cytochrome c oxidase on reduction and on ligand binding, Biochim. Biophys. Acta 1186 (1994) 19–26.
[81] E. Forte, M.C. Barone, M. Brunori, P. Sarti, A. Giuffre, Redox-linked protonation of cytochrome c oxidase: the effect of chloride bound to CuB, Bichemistry 41 (2002) 13046–13052.
[82] E. Forte, F.M. Scandurra, O.-M.H. Richter, E. D'Itri, P. Sarti, M. Brunori, B. Ludwig, A. Giuffre, Proton uptake upon anaerobic reduction of the paracoccus denitrificans cytochrome c oxidase: a kinetic investigation of the K354M and D124N mutants, Biochemistry 43 (2004) 2957–2963.
[83] V. Sharma, M. Wikstrom, The role of the K-channel and the active-site tyrosine in the catalytic mechanism of cytochrome c oxidase, Biochim. Biophys. Acta 2016 (1857) 1111–1115.
[84] M.R.A. Blomberg, The structure of the oxidized state of cytochrome c oxidase - experiments and theory compared, J. Inorg. Biochem. 206 (2020), 111020.
[85] A. Tuukkanen, M.I. Verkhovsky, L. Laakkonen, M. Wikstrom, The K-pathway revisited: a computational study on cytochrome c oxidase, Biochim. Biophys. Acta (2006) 1117–1121.
[86] M.R.A. Blomberg, The redox-active tyrosine is essential for proton pumping in cytochrome c oxidase, Front. Chem. 9 (2021), 640155.
[87] A. Shimada, F. Hara, K. Shinzawa-Itoh, N. Kanehisa, E. Yamashita, K. Muramoto, T. Tsukihara, S. Yoshikawa, Critical roles of the Cu(B) site in efficient proton pumping as revealed by crystal structures of mammalian cytochrome c oxidase catalytic intermediates, J. Biol. Chem. 297 (2021), 100967.
[88] E.A. Gorbikova, K. Vuorilehto, M. Wikstrom, M.I. Verkhovsky, Redox titration of all electron carriers of cytochrome C oxidase by fourier transform infrared spectroscopy, Biochemistry 45 (2006) 5641–5649.
[89] F. Kruse, A.D. Nguyen, J. Dragelj, J. Heberle, P. Hildebrandt, M.A. Mroginski, I. M. Weidinger, A resonance raman marker band characterizes the slow and fast form of cytochrome c oxidase, J. Am. Chem. Soc. 143 (2021) 2769–2776.
[90] M. Wikstrom, R. Springett, Thermodynamic efficiency, reversibility, and degree of coupling in energy conservation by the mitochondrial respiratory chain, Commun. Biol. 3 (2020) 451.
[91] N. Yano, K. Muramoto, A. Shimada, S. Takemura, J. Baba, H. Fujisawa, M. Mochizuki, K. Shinzawa-Itoh, E. Yamashita, T. Tsukihara, S. Yoshikawa, The Mg2+-containing water cluster of mammalian cytochrome c oxidase collects four pumping proton equivalents in each catalytic cycle, J. Biol. Chem. 291 (2016) 23882–23894.